Proceedings World Geothermal Congress 2026
Calgary, Canada, June 8 – 11, 2026

Investigation Of Fine Particles Mobilization During Geothermal Production From The Anglo-Paris Basin Albian Aquifer Using Coreflooding Experiments

E. Rao[1], D. Rousseau[1]*, R. Deschamps[1], F. Seguin[1] and J. Poulizac[1]
[1]: IFP Energies nouvelles, 1 avenue de Bois Préau, 92852 Rueil-Malmaison, France
david.rousseau@ifpen.fr

Keywords: Albian reservoir, reinjection, injectivity decline, coreflooding, fine particles

ABSTRACT

This study investigated the mobilization of fine particles during geothermal production from the Anglo-Paris Basin Albian aquifer, that is suspected to entail injectivity decline at the reinjection side. It involved coreflooding experiments performed with clayey sand samples from Albian-aged "Greensand" formation. Sandpacks were prepared in a core holder equipped with a downstream filter and exposed to flow velocities varying from 0.3 m/day (in-depth aquifer flow) to about 200 m/day (near wellbore flow). The injection tests were performed primarily with a low salinity synthetic water representative of the aquifer (TDS = 0.17 g/L) and also with a high salinity water, to mimic the exposure of the near wellbore sediments to drilling fluids. The pressure drops across the porous medium and the downstream filter were recorded during injection. The filters were collected after each velocity or salinity step and analysed by SEM (images, chemical analysis) and XRD. At low and intermediate velocities, moderated particle production was observed. After a threshold velocity, massive particle production occurred and was associated to changes of the composition balance between clays and silica. Moreover, even for sandpacks primarily exposed to Albian water injection at low to high velocity, a salinity chock towards the high salinity water led, surprisingly, to additional and very significant particle production. These results show that both hydrodynamic and complex physicochemical interactions play a role in controlling particle release. They could help setting up new specifications for the production rates and well diameters as well as for the composition of the drilling fluids.

1 INTRODUCTION

In the course of operating a geothermal wells doublet, injectivity decline corresponds to the increase in injection pressure associated with the decrease in the geological formation's capacity to accept the reinjected fluid. By inducing a reduction in production flow rate and, consequently, in thermal power, injectivity decline compromises the economic profitability of the doublet. This phenomenon is particularly significant in clastic reservoirs, where the flow takes place in the porous matrix with pore throat sizes measured in microns. It has been observed in numerous geothermal doublets in clastic reservoirs worldwide (Ungemach, 2003; Kamila et al., 2021; Song et al., 2020; Luo et al., 2023), and several operations have been compromised or, in some cases, abandoned. For example, one can cite the case of the Triassic formations of the Paris Basin: in these consolidated clay-sandstone formations with a complex and heterogeneous sedimentary architecture, there were three failures in the operations of Melleray, Cergy, and Achères in France (Bugarel et al., 2018).

The mechanisms responsible for injectivity decline are related either to the presence of particles in the injected water or to a modification of the in-situ formation caused by reinjection. They can be grouped into four categories (Burté, 2018; Raies et al., 2023): (i) corrosion, including bacterial corrosion and biofilm formation; (ii) fluid destabilization (precipitation of chemical species due to variations in pressure, temperature, pH, and/or composition); (iii) geochemical phenomena of fluid-rock interactions; and (iv) the detachment of fines (namely mineral particles smaller than the main sand grains) from the formation, leading to their deposition either in the formation at the reinjection point or in the conduits, particularly in heat exchangers.

This study addresses the question of fines detachment occurring in the formation near the production well of a geothermal doublet. It focuses on the Albian-aged "Greensands" from the Anglo-Paris Basin, using as a reference case the geothermal doublets of the "ZAC du Moulon" on the Saclay plateau in France (depth: 700m, produced water temperature: 31°C). These doublets have experienced injectivity issues that have been the subject of several experimental studies and remediation attempts (Maurel et al., 2020; Boujlel et al., 2023). The experimental approach in this work consists in performing coreflood tests where Albian aquifer sand samples are exposed to water flow velocities and salinity changes representative of the near wellbore conditions, and in analyzing the released particles collected at the outlet of the porous media.

2 GEOLOGICAL CONTEXT

2.1 Stratigraphic and Structural Evolution of the Anglo-Paris Basin During the Aptian–Albian Interval

The Anglo-Paris Basin comprises several sub-basins initiated during the Carboniferous and Permian periods. These sub-basins are structurally bounded by major faults inherited from the Variscan orogeny and subsequent collapse. The reactivation of these inherited structures produced variable tectono-stratigraphic responses throughout the Mesozoic, particularly during the extensional regime of the Lower Cretaceous (Figure 1).

The northern sector of the Anglo-Paris Basin consists of four distinct sub-basins—Channel, Winterborn-Kingston, Vale of Pewsey, and Weald—separated by Variscan fault systems (Evans et al., 2003). Collectively, these sub-basins constitute the Wessex Basin. In contrast, the southern sector is characterized by a more homogeneous sub-basin, corresponding to the Paris Basin sensu stricto.

The Aptian–Albian sedimentary succession within the Paris Basin predominantly reflects shallow to open marine depositional environments, with localized occurrences of continental and deltaic facies along basin margins (Guillocheau et al., 2000; Deconinck et al., 2021). While the Lower Cretaceous is marked by significant exhumation of the Armorican Massif and Massif Central (Barbarand et al., 2001; François et al., 2020; Olivetti et al., 2020), the southeastern portion of the Anglo-Paris Basin likely remained open toward the Tethyan realm, extending across present-day Burgundy and further eastward (Amédro et al., 2023).

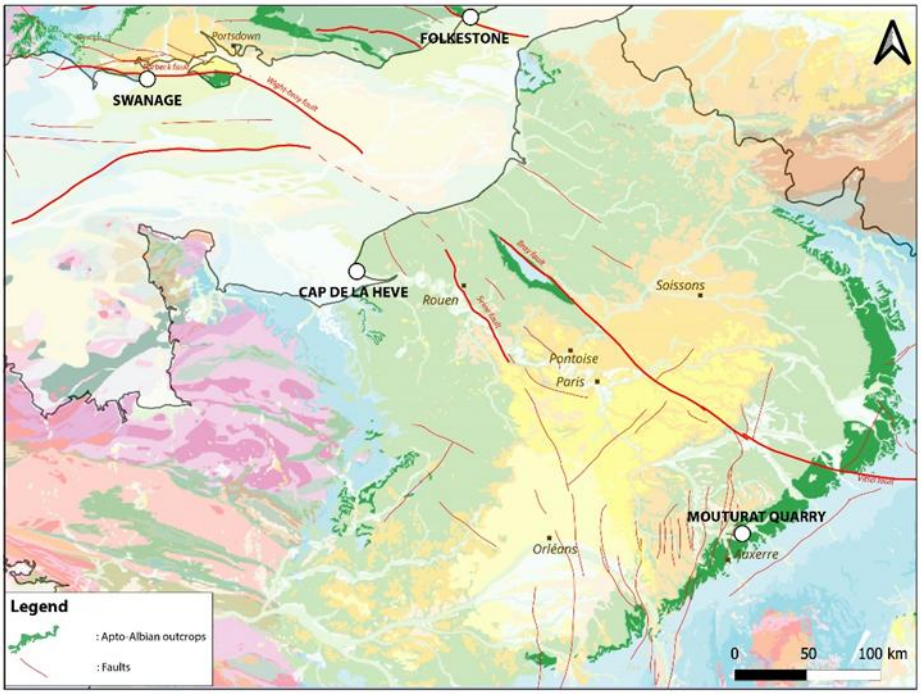


Figure 1: Location maps of the sections where samples were taken.

2.2 Lithographic framework

The sedimentary succession of the Aptian-Albian deposits is summarized in Figure 2, and described as follow:

2.2.1 Argiles à Plicatules Formation (Lower Aptian)

Deposited atop Barremian continental strata, the Argiles à Plicatules Formation records a marine transgression from the southeast that inundated much of the Paris Basin. These deposits consist of dark green marine clays rich in large Plicatula bivalves, indicative of a calm, open marine setting. Peripheral truncation due to Late Aptian erosion is observed (Mas, 2024; Guillocheau et al., 2000).

2.2.2 Sables Verts Formation (Upper Aptian)

The Sables Verts sensu stricto were emplaced during a progressive transgression within a tidally influenced littoral system under conditions of low subsidence (Guillocheau et al., 2000). These glauconite-rich sands overlie an erosional unconformity marking the Upper Aptian sequence boundary, associated with regional uplift during the Bay of Biscay rifting event (Amédro et al., 2017; Mansy et al., 2003). The formation comprises three transgressive sequences, each corresponding to distinct sedimentary prisms (Amédro et al., 2023).

In the Aube region, Lower Albian facies of the Sables Verts exhibit upward-fining glauconitic sands with clay-rich interbeds in the lower third (Amédro et al., 2017). The formation is overlain by the Argiles de l'Armance (Lower Albian), which serve as a transitional unit between the Sables Verts and the Sables des Drillons formations.

2.2.3 Sables des Drillons Formation (Lower Albian)

Deposited during a phase of relative sea-level fall, the Sables des Drillons Formation reflects a regressive system tract characterized by lowstand sandy lobes within a fluvially dominated deltaic environment (Sévenier & Lasseur, 2016). Rich in Otohoplites ammonites, the sequence thins eastward and transitions distally into the Argiles de Courcelles Formation, indicative of a shift to offshore depositional settings (Amédro & Matrion, 2014).

2.2.4 Argiles Tégulines de Courcelles Formation (Lower to Middle Albian)

Dominant in the northeastern basin, this formation comprises offshore marine clays overlying the Sables des Drillons interval (Amédro & Matrion, 2014).

2.2.5 Sables de Frécambault Formation (Middle Albian)

Associated with a major paleogeographic reorganization (Sévenier & Lasseur, 2016), these clean shoreface sands were rapidly deposited in a wave-dominated shallow marine environment. Notably coarse and low in glauconite, they extend into the Aube and thin northeastward, laterally interfingering with the Argiles Tégulines facies.

Toward the east, the Argiles des Pommerats dominate, while sandier facies prevail in the western regions including Yonne, Puisaye, and Sancerrois (Amédro & Matrion, 2014).

2.2.6 Argiles de Gault Formation (Upper Albian)

The Gault Clay Formation is widespread across the Anglo-Paris Basin. In the Aube region, it is associated with the Marnes de Brienne and records a major marine flooding event, particularly pronounced in the western Paris Basin (Bomou et al., 2016).

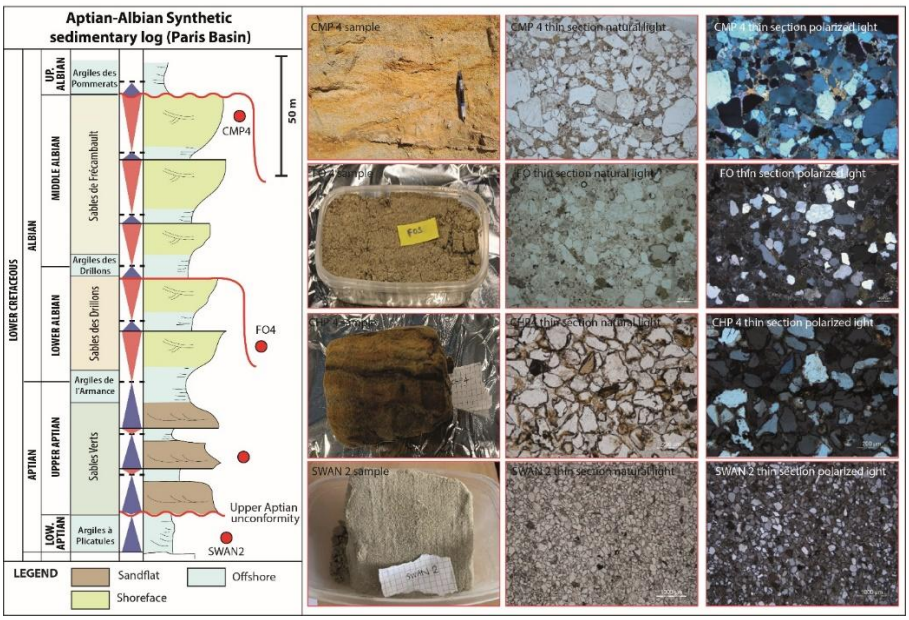


Figure 2: Synthetic sedimentary column of the Aptian-Albian deposits in the Paris Basin with samples picture and stratigraphic position.

3 MATERIALS AND METHODS

3.1 Albian aquifer sand samples

The samples tested in the coreflood experiments are representative of the Albian aquifer and the stratigraphic formation of the greensands, each sample set thus provides a representative cross-section of unconsolidated and poorly consolidated sands from different Aptian to Albian outcrops across France and England (see Figure 2 and Table 1).

3.1.1 Samples CHP4/CHP5: Consolidated ferruginous sands from the Upper Aptian Greensands Formation. These samples were obtained from the Cap de la Hève site in Normandy, France. Those ferruginous

sands correspond to a tidal bar facies - sandy sedimentary body formed in tide-dominated environments;

3.1.2 CM4: Poorly consolidated sands from the Sables de Frécambault Formation, Middle Albian age. These samples were collected at the Mouturat Quarry, locally known as "Les Sablonnières", in the town of St Florentin. The Frécambault sands are associated with mouth bar facies. A mouth bar facies refers to deposits that form where a river enters a standing body of water (such as a sea or lake), leading to rapid deceleration of flow and the accumulation of sandy to silty sediments in a bar-shaped geometry;

3.1.3 SWAN2: Unconsolidated English ferruginous sand of Lower Aptian age, collected at Swanage, England. Its facies correspond to a tidal bar.

Table 1: Characteristics of the samples used for the coreflood experiments.

Sample name	Location	Formation	Age	Sample type	Facies
CM4	St Florentin (Bourgogne)	Sables de Frécambault	Middle Albian	Poorly consolidated sands	Mouth bar
CHP4	Cap de la Hève (Normandie)	Sables Verts	Upper Aptian	Consolidated ferruginous sands	Tidal Dune
CHP5					
SWAN2	Swanage (Wessex)	Lower Greensands	Lower Aptian	Non-consolidated ferruginous sands	Tidal Dune

3.2 Waters

Two synthetic waters were used in the experiments, of which the composition is presented in Table 2. The "Albian" water was a simplified synthetic water representative of the low salinity reservoir water of the geothermal site of Saclay, according to a produced water analysis performed by Eurofins Hydrologie Ile-de-France in 2018 (private communication). The "Albianx1000" brine was prepared by multiplying by 1000 the mass concentration of all components of the "Albian" water. It is meant to represent the brines to which the near wellbore area can be exposed during drilling with water-based mud or workovers. As no representative compositions of such brines were available, multiplying the salts concentrations in Albian water was considered the most relevant approach. Both waters have the same hardness parameter of 0.74 (defined as the ratio of the mass concentration of calcium and magnesium cations over the mass of concentration of all four cations), which is very high. As a result, the "Albian x1000" brine is, at the same time, a high salinity water (170 g/L total dissolved solids) and a very hard water. The pH of the waters was not controlled and was hence close to neutrality and slightly acidic, as usual for water at equilibrium with air are ambient conditions.

Table 2: Composition of the waters investigated.

Ion	Concentration in synthetic "Albian" water (mg/L)	Concentration in "Albian x1000" brine (mg/L)
Na+	6.8	6 800
K+	9.3	9 300
Ca2+	37.0	37 000
Mg2+	8.2	8 200
Cl-	108	108 301
Total Dissolved Solids	**0.170**	**169 601**

3.3 Exploratory tests in static conditions

Prior to the coreflood experiments, exploratory bottle tests were performed to qualitatively investigate the impact of exposing the Albian sands to high salinity. For these tests, about 20g of each sand investigated were first dried at 40°C and then immersed in bottles of about 75 mL of either Albian or Albianx1000 water and gently shaken by turning them downwards 3 times. They were then left to rest for 10 minutes before pictures were taken.

3.4 Experimental setup for the coreflood experiments

The coreflood tests aimed at investigating the impact of velocity and salinity changes on particles destabilization and release, in terms of overall amount and composition in clays vs. quartzic matter. Prior to each experiment performed with Albian unconsolidated rock, the sand sample was dried at 40°C, then gently grounded with a mortar and pestle made from hard, non-porous agate stone (valued for its ability to finely grind samples without introducing impurities) and sieved at 500 µm. These steps allowed to remove agglomerates while preserving the integrity of the individual grains. The sand was then dry-packed in a core-holder made of Peek of 3 cm inner diameter, closed with pistons equipped with Nylon grids of 30 µm mesh opening. This led, for all of the Albian sand samples, to porosities of 44±1%, as determined by weighting of the core holder and using a grain density,

determined with a helium pycnometer, of 2.66 g/cm3 (which was found to be identical for all samples). For comparison purposes, two experiments were also performed with a Fontainebleau-type sand made of more than 99% quartz by weight (GA39 from Sibelco/Sifraco). The porosity for the GA39 sand packs was of 41%, calculated by weighting with a measured grain density of 2.65 g/cm3. The GA39 sand is made of large grains of typical size 100 µm on which fine, micron-sized, particles are attached. For the first experiment with GA39, the sand was treated by repeated washes in alkaline water (NaOH solution, pH≈9) to detach the fine particles (Rousseau et al., 2008). For the second experiment, the sand was untreated, hence fine particles were prone to detach upon hindering of the charge-screening effect caused by a reduction of salinity. The length of all porous media was about 14 cm.

A custom coreflood setup was built for the experiments (Figure 3). Upstream the porous medium, two volumetric pumps (QX6000 from Chandler) injecting degassed water kept under argon atmosphere and a 4 ways valve were set to enable injection of water at various flow rates and to switch from one water to another. The lines connected to the two pumps were equipped with cellulose ester filters of 0.22 µm mesh opening (MF-type from Millipore) to avoid injecting any unwanted particle that could remain in the waters. Downstream the porous medium, a filters stack was installed to collect the particles exiting the porous medium. The stack was made of a 0.22 µm (MF-type from Millipore) set to hold the main filter and a main filter made of fiberglass (also from Millipore) with 1 µm mesh opening. Fiberglass was chosen as it was deemed compatible with SEM analysis. The tubing between the outlet of the porous medium and the filter stack was made of transparent FEP of 1.6 mm inner diameter and with a length of 10 cm. The porous medium and filter stack assembly was vertical, with the filter stack set below. Both the porous medium and the filter stack were equipped with differential pressure sensors (DS265 from ABB) with 400 mbar and 60 mbar measurement range, respectively for the porous medium and the filter stack.

The temperature of the Albian aquifer varies depending on location and depth, ranging from 18 °C to 36 °C (Hervé and Ignatiadis, 2007). For the experiments performed in the present work, it was decided to work at ambient temperature of 21±1°C.

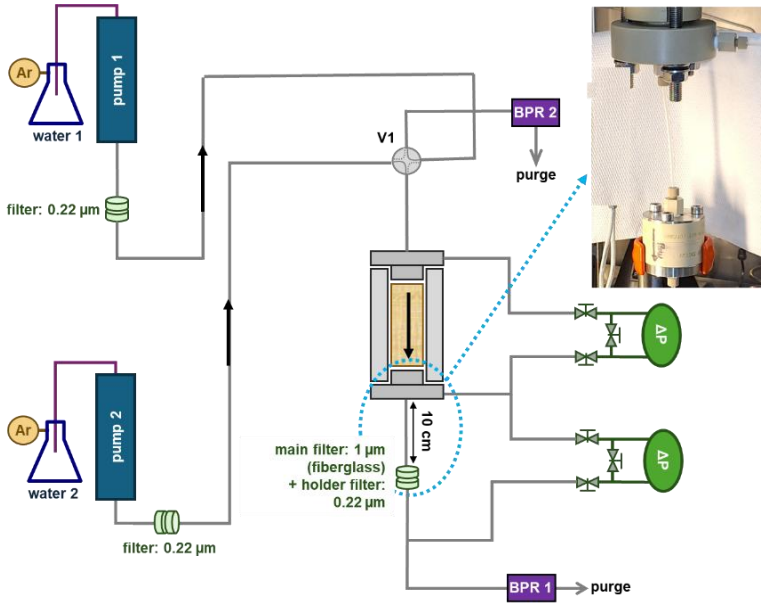


Figure 3: Experimental setup with picture of the tubing and filter cell set downstream the porous medium.

3.5 Analytical techniques

The fiber glass filters collected after each step of each coreflood experiments were analyzed at first by direct visual observation and then by SEM, performed on a Zeiss CrossBeam system. This approach enables detailed visualization of particle size, shape, and textural features, critical for identifying fine particles mobilized during the coreflood experiments. Prior to imaging, filter samples were metallized with a thin carbon coating of a few nanometers thickness to enhance surface conductivity and improve image resolution by reducing charging effects.

3.6 Experimental parameters and procedures

3.6.1 Saturation and characterization of the porous media

For the experiments performed with the GA39 sand, which is made of stable quartz particles with respect to varying hydrodynamic forces, a conventional vacuum-saturation method was employed. After dry-packing the

sand, vacuum was created in the core holder using a rotary vane pump for 2 hours, then degassed water was introduced at atmospheric pressure. After mounting the core holder in the setup and maintaining a continuous injection of degassed water for at least one night with the volumetric pump, permeability was determined by varying the injection flow rate. It was found to be of 4.4 and 5.7 Darcy, respectively for the treated and the untreated sand.

For the experiments performed with the Albian sands, which are made of a priori unstable quartz and clay particles, an adapted saturation procedure had to be implemented. At first, the core holder containing the dry packed sand was mounted in the setup, then at least three times the pore volume of water was injected at the lowest velocity of the range investigated (see next section). Permeability could not be due to particles instability, but the order of magnitude of the pressure drops measured showed that it was clearly in the multi-Darcy range.

3.6.2 Injection velocities

For the experiments with the Albian sands, the injection interstitial velocities investigated varied from an initial low velocity typical of in-depth reservoir flow to a much higher velocity representative of near wellbore conditions. The initial saturation velocity was hence 0.31 m/day (corresponding to a volumetric flow rate of 4 mL/h) and was then stepwise increased by a factor of 5. Namely, the velocities investigated were: 1.56, 7.81, 39.0 and 195 m/day. For the experiments with the GA39 sand, the injection velocity was set to 1.56 m/day.

3.6.3 Procedures and experimental plan

The list, main conditions and objective of the coreflood experiments performed is presented in Table 3.

The experiments with the GA39 sand aimed at assessing the impact of decreasing salinity on the release of fine quartz particles from the main quartz grains, in the absence of any clay particles. The porous media were hence initially saturated with the Albianx1000 brine and the Albian water was injected in a second step. A first reference experiment was performed with the treated GA39 sand (CF01, GA39 no fines) and then the main experiment was performed with the untreated GA39 sand (CF02, GA39 with fines). In these experiments the main observables were the pressure drops. As the quartz particles on the downstream filters were in low amount and not distinguishable from the glass fibers, analysis of the collected filters did not bring any useful information.

Table 3: Overview of the coreflood tests performed.

Exp. #	Porous medium	Initial saturation water	Objective
CF01	GA39 no fines	Albian x1000	impact decreasing salinity shock
CF02	GA39 with fines	Albian x1000	impact decreasing salinity shock
CF03	CM4	Albian	impact flow rate & increasing salinity shock
CF04	SWAN2	Albian	impact flow rate & increasing salinity shock
CF05	CHP4/CHP5	Albian	impact flow rate & increasing salinity shock

The experiments with the Albian sands aimed at assessing, at first, for the impact of varying flow velocities on particle release in salinity representative of the reservoir water and, second, for the impact of increasing salinity at velocity representative of near wellbore conditions. The porous media were hence initially saturated with Albian water, then the velocity was stepwise increased and finally, after reaching the maximum velocity, the injection water was abruptly changed to Albianx1000 brine. After each step within each experiment, the downstream filter wad collected, dried at 40°C and analyzed visually and by SEM and a new filter was installed for the next step. Given that the structure of the porous media was strongly altered due to massive displacement of large particles at each step, the pressure drops measurements proved to be unusable. Experiments CF03, CF04 and CF05 were performed respectively with samples CM4, SWAN3 and CHP4/CHP5.

4 RESULTS AND DISCUSSION

4.1 Exploratory tests in static conditions

The results presented in Figure 4 for the Albian sand samples CHP4/CHP5 and SWAN2 show that the supernatant phase is more turbid in Albianx1000 than in Albian water, indicating that either more or smaller particles are released in the higher salinity environment. Such behavior appears a priori surprising as, according to the classical theory of colloidal stability and double-layer compression (Israelachvili, 2011), expectations are that lower salinity conditions enhance the dispersion of clay particles. Indeed, in dilute solutions, the diffuse electrical double layer surrounding negatively charged clay particles is more extended, leading to greater inter-

particle repulsion and thus a more stable suspension. In contrast, high salinity compresses the double layer due to increased ionic strength, allowing van der Waals forces to dominate ("charge screening" effect), which promotes flocculation and sedimentation.

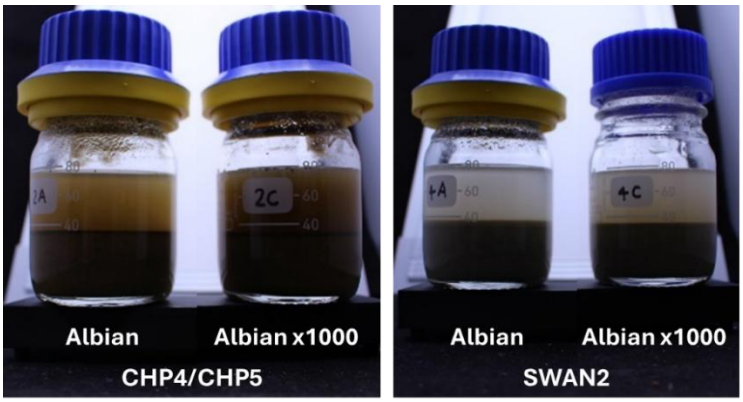


Figure 4: Results of the qualitative static tests where CHP4/CHP5 (left) and SWAN2 (right) sands were exposed to synthetic Albian and Albianx1000 water.

The present experimental results suggests that additional mechanisms are influencing the behavior of the fine fractions. According to Le and coworkers (Le, 2024), for kaolinite and other clay minerals, the presence of salts such as NaCl can lead to the formation of numerous small aggregates rather than fewer, larger, and more compact ones. These smaller aggregates increase the total surface area exposed to the solvent and remain suspended longer, thus increasing turbidity. This phenomenon is attributed in particular to the anisotropic shape of clay particles and the heterogeneity of surface charges. Moreover, at certain salinity levels, the ionic environment may promote the stabilization of these smaller aggregates, preventing their further coalescence into larger flocs. This effect can be exacerbated by the presence of divalent or trivalent cations, or by specific ion adsorption, which modifies surface charge distribution and interparticle interactions.

4.2 Reference tests with quartzic sand

In the first test CF01, performed with GA39 sand from which the fine particles had been removed, no change in pressure drops were recorded, across the porous media and the downstream filter, upon abruptly decreasing the salinity from Albianx1000 to Albian water. In the second test, CF02 with fines-bearing GA39 sand, marked pressure increase were recorded upon salinity decrease. As shown in Figure 5, the pressure drop across the porous medium slightly increased from the beginning of the Albian water injection (set as a the "0" of the x-axis labelled as number of pore volumes of Albian water injected) and the pressure drop across the filter started to increase after having injected 1 pore volume (the dead volume of tubing between the outlet of the porous medium and the filter being subtracted on the x-axis scale). This indicates that particles displacement takes place in the porous medium when the low salinity front propagates and that particles are released from the porous medium when the front reaches its outlet, leading to a partial plugging of the filter.

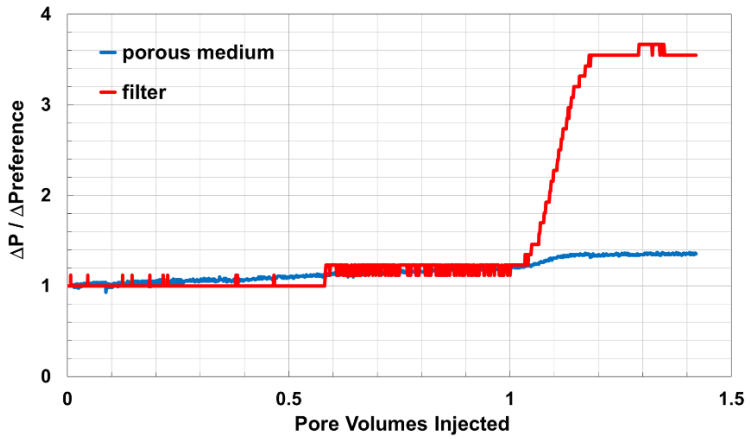


Figure 5: Results of coreflood tests CF02 (untreated as normalized pressure drops across the porous medium and across the filter) versus the volume of Albian brine injected normalized as number of pore volumes injected.

These results stand as references showing that, with the experimental setup and the experimental procedure implemented in this study and when only quartz particles are present, fine particles release takes place as expected based on classical charge screening effects reduction upon salinity change, as widely reported in the literature for quartz particles which are negatively charged at pH close to neutrality (Khilar and Fogler, 1998). This confirms that the opposed behavior observed with the Albian sands (in the static bottle tests and in the coreflood tests discussed in the next section) is to be attributed to clay particles.

4.3 Impact of velocity and salinity changes for various mineralogies

Figure 6 shows the results of the 3 coreflood tests performed with the Albian sands in terms of visual aspect of the individual fiber glass filters collected after each step within each experiment, namely the initial injection velocity of 0.31 m/day used for saturation with Albian water, then the stepwise increase of velocity until the typical near wellbore velocity of 195 m/day and then the abrupt increase of salinity to Albianx1000 brine, still at 195 m/day. The first major observation is that the same overall trends take place for all sand samples investigated. Regarding the impact of injection flow rate, the results show that: (i) at the saturation velocity, an initial release of fines takes place which is likely due to fines that were not or poorly attached to the main grains, (ii) up to 7.81 m/day (for CM4 in CF03) or 39.0 m/day (for SWAN2 in CF04 and CHP4/CHP5 in CF05), no additional release occurs, (iii) above these velocity thresholds, massive release of fines takes place. Such thresholds evidence that strong enough hydrodynamic forces are required to pull-out fines by overcoming their adhesion energy. The most surprising result is that the salinity shock towards Albianx1000 brine at high velocity leads to a massive additional release of fines. This shows that physicochemical parameters strongly influence the adhesion energy. Namely, the adhesion energy seems to decrease when salinity increases.

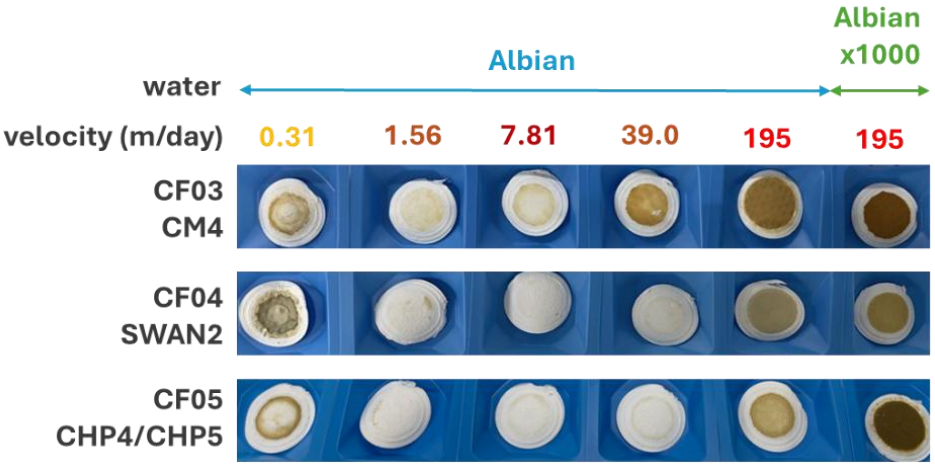


Figure 6: Visual aspect of the main filters collected downstream of the porous medium after each step of each experiment performed.

The SEM observations allowed to further investigate the fine particles release mechanism. Figure 7 shows the SEM images of the fiber glass filters collected during the increasing velocity steps in experiment CF04 with sand CM4. The morphology of the particles suggests that, at low velocity, the particles released are mainly made of quartz, whereas, above the pull-out threshold, the particles released are mainly made of clays. The release of quartz particles even when hydrodynamic forces are very low is not surprising given the low salinity context. It is consistent with the outcomes of the test with GA39 quartzic sand. Namely, in the absence of charge screening effect, electrostatic repulsion of the negatively charged quartz surfaces dominates over Van der Waals attraction. The fact that pulling-out clay particles requires higher hydrodynamic forces suggests that these particles either have stronger attractive energy, or bear only little electric charges, or both.

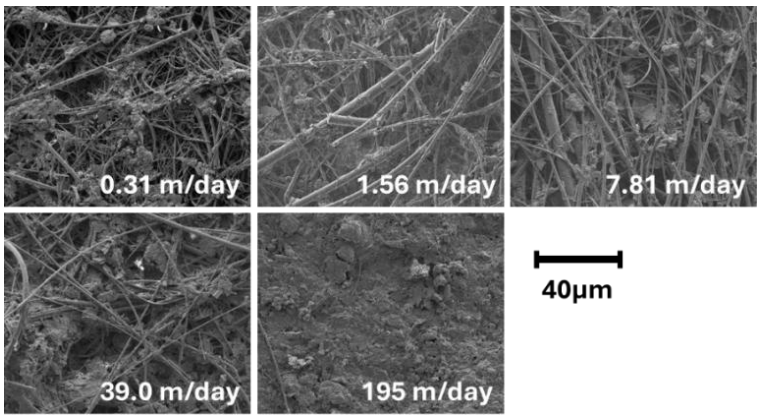


Figure 7: Aspect from SEM analysis of the main filters collected during the velocity increase steps in Albian water of the coreflood experiments, example shown for test CF04, performed with sand CM4.

Figure 8 shows the SEM images of the fiber glass filters collected during the increasing velocity steps in experiment CF05, performed with sand CHP4/CHP5. It clearly appears that the particles that are massively released during the salinity shock are made of clay. This result is compatible to that of the static bottle tests, which showed that clays particles are smaller, hence more self-repulsive and less strongly attached onto the main grains, in high salinity environment. The absence of quartz on the filter is consistent with the fact that all

fine quartz particles present where already released due to electrostatic repulsion in the initial low salinity environment.

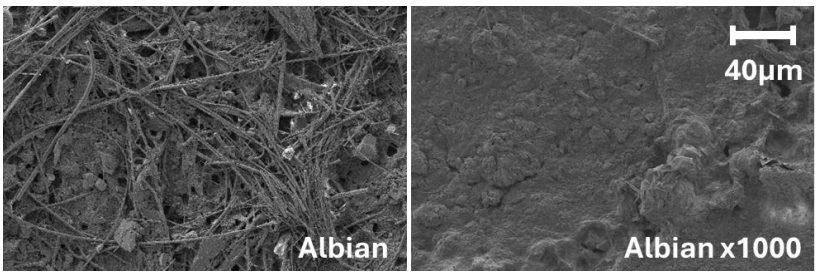


Figure 8: Aspect from SEM analysis of the main filters collected during the salinity change steps at injection velocity of 195 m/day of the coreflood experiments, example shown for test CF05, performed with sand CHP4/CHP5.

5 CONCLUSION

The results of this exploratory experimental study show that both hydrodynamics and complex physicochemical interactions play a role in controlling fine particle release from Albian sands in conditions representative of the near-wellbore environment of the actual industrial operations. The stepwise velocity increase study in the low-salinity Albian aquifer water revealed the presence of velocity thresholds for the release of clay fines, evidencing that strong enough hydrodynamic forces are required to pull-out the particles by overcoming their adhesion energy. The salinity shock study, performed in order to assess for the impact of the potential exposure of the formation near the wellbore to high salinity drilling or workover fluids, revealed, surprisingly, that a salinity increase led to massive additional destabilization of the clays.

These results need to be complemented by a more systematic study involving porous media made of controlled and well quantified clay species as well as brines more representative to that employed during drilling or workovers. However, they set the ground for setting up new specifications for the production rates and well diameters (impacting velocity) as well as for the composition of the drilling and workover fluids.

Acknowledgement

The authors are grateful to IFPEN for founding this work and for authorizing its publication.

REFERENCES

Amédro, F., Matrion, B. (2014). L'étage Albien dans sa région-type, l'Aube (France): une synthèse dans un contexte sédimentaire global. Carnets De Géologie (Notebooks on Geology), 14(5). https://doi.org/10.4267/2042/53732

Amédro, F., Matrion, B., Deconinck, J.-F., Huret, E., Landrein, P. (2017). Les forages de Juzanvigny (Aube, France): litho-biostratigraphie des formations du Barrémien à l'Albien moyen dans l'est du bassin de Paris et datations par les ammonites. Geodiversitas, 39(2), 185–212. https://doi.org/10.5252/g2017n2a2

Amédro, F., Deconinck, J.-F., Ferry, S., Landrein, P. (2023). Les formations du Crétacé inférieur (Berriasien/Valanginien à Albien) du département de l'Aube (Est du Bassin parisien) : lithostratigraphie et environnements de dépôt. Géologie De La France, 3, 36–62.

Barbarand, J., Lucazeau, F., Pagel, M., Séranne, M., 2001. Burial and exhumation history of the south-eastern Massif Central (France) constrained by apatite fission-track thermochronology. Tectonophysics 355 (3–4), 275–290.

Bomou, B., Deconinck, J.-F., Pucéat, E., Amédro, F., Joachimski, M. M., Quillévéré, F. (2016). Isotopic seawater temperatures in the Albian Gault Clay of the Boulonnais (Paris Basin): palaeoenvironmental implications. Proceedings of the Geologists' Association, 127(6), 699–711. https://doi.org/10.1016/j.pgeola.2015.08.005

Boujlel J., Souque C., Rousseau N., Nabzar L., Deschamps R. and Ungemach P. (2023): "Reinjection Problematic in Poorly Consolidated Geothermal Reservoirs. Laboratory investigations", World Geothermal Congress, proceedings.

Bugarel F., Bouchot V. and Barrière J. (2018): "Projet GUIDOCLAST. Guide de bonnes pratiques pour une exploitation optimale et durable d'opérations géothermiques de basse température en réservoir argilo-gréseux ou sableux", rapport ADEME–BRGM, BRGM/RP-67113-FR, http://infoterre.brgm.fr/rapports//RP-69790-FR.pdf (2018)

Burté L. (2018): "Etude des risques de colmatage et optimisation des processus de traitement des doublets géothermiques superficiels", Thèse de l'Université de Rennes, https://theses.fr/2018REN1B019.

Deconinck, J.F., Boué, D., Amédro, F., Baudin, F., Bruneau, L., Huret, E., Landrein, P., Moreau, J.D., Santoni, A.L. (2021). First record of early Aptian Oceanic Anoxic Event 1a from the Paris Basin (France) - Climate signals on a terrigenous shelf. Cretaceous Research 125 (2021) 104846. https://doi.org/10.1016/j.cretres.2021.104846.

Deconinck, J.F., Boué, D., Amédro, F., Baudin, F., Bruneau, L., Huret, E., Landrein, P., Moreau, J.D., Santoni, A.L. (2021). First record of early Aptian Oceanic Anoxic Event 1a from the Paris Basin (France) - Climate signals on a terrigenous shelf. Cretaceous Research 125 (2021) 104846. https://doi.org/10.1016/j.cretres.2021.104846.

Guillocheau, F., Robin, C., Allemand, P., Bourquin, S., Brault, N., Dromart, G., Friedenberg, R., Garcia, J.P., Gaulier, J.M., Gaumet, F., Grosboy, B., Hanot, F., Le Strat, F., Mettraux, M, Nalpas, T., Prijac, C., Rigolet, C., Serrano, O., Grandjean, G. (2000). Meso-Cenozoic geodynamic evolution of the Paris Basin: 3D stratigraphic constraints. Geodinamica Acta, 13(4), 189–245. https://doi.org/10.1080/09853111.2000.11105372.

Hervé, J.Y. and Ignatiadis I. (2007). "Nappes de l'Albian et du Néocomien, Définition des conditions d'accès à la ressource géothermique en Ile-de-France", BRGM report 55990-FR, http://infoterre.brgm.fr/rapports/RP-55990-FR.pdf

Israelachvili, J.N. (2011): "Intermolecular and Surface Forces", Third Edition, Academic Press.

Kamila Z., Kaya E., Zarrouk S.J. (2021): "Reinjection in geothermal fields: An updated worldwide review 2020", Geothermics, 89, 101970, https://doi.org/10.1016/j.geothermics.2020.101970

Khilar K.C. and Fogler H.S. (1998). "Migrations of Fines in Porous Media", Springer Dordrecht, https://doi.org/10.1007/978-94-015-9074-7

Le, TTB, Finney, A.R., Zen, A., Bui, T., Tay, W.J., Chellappah, K., Salvalaglio, M., Michaelides, A. and Striolo, A. (2024): "Mesoscale Simulations Reveal How Salt Influences Clay Particles Agglomeration in Aqueous Dispersions", J. Chem. Theory Comput., 20, 1612−1624, https://doi.org/10.1021/acs.jctc.3c00719

Luo W., Kottsova A., Vardon P.J., Dieudonné A.C. and Brehme M. (2023): "Mechanisms causing injectivity decline and enhancement in geothermal projects", Geothermics, 185, 113623, https://doi.org/10.1016/j.rser.2023.113623

Mas, P. (2024). Géothermie dans les réservoirs silico-clastiques : Apport de l'étude d'un analogue de terrain (Grès de Roda) pour la modélisation des hétérogénéités sédimentaires du réservoir argilo-sableux de l'Albien du Bassin de Paris. Université Paris-Saclay, Saclay.

Maurel, C., Bugarel, F. and Hamm, F. (2020): "Retour d'expérience des opérations de géothermie à l'Albien et au Néocomien du Bassin de Paris", BRGM report RP-69427-FR, http://infoterre.brgm.fr/rapports/RP-69437-FR.pdf

Olivetti, V., Balestrieri, M., Godard, V., Bellier, O., Gautheron, C., Valla, P.G., Zattin, M., Facenna, C., Pina Jamma, R., Manchuel, K. (2020). Cretaceous and late Cenozoic uplift of the eastern French Massif Central: insights from low- temperature thermochronometry. Lithosphere, 2020, 12 ((1)), pp.133-149. ff10.1130/L1142.1ff. ffhal-02464552f.

Raies I., Fleury M., Kohler E., Pédel N. and Ledésert B. (2023): "Formation damage induced by clay colloids deposition in Triassic clastic geothermal fields: Insights from an experimental approach", Applied Clay Science, 234, 106868, https://doi.org/10.1016/j.clay.2023.106868

Rousseau, D., Hadi, L. and Nabzar, L. (2008). PWRI-Induced Injectivity Decline: New Insights On In-Depth Particle Deposition Mechanisms. SPE Production & Operation, 23(04), pp. 525-531, SPE-107666-PA, https://doi.org/10.2118/107666-PA

Sévenier, M., Lasseur E. (2016). Géométries 3D et variations latérales des dépôts albiens du bassin de Paris. Continuité des réservoirs sableux et intégrité des niveaux argileux. BRGM/RP-66377-FR.

Song W., Liu X., Zheng T. and Yang J. (2020): "A review of recharge and clogging in sandstone aquifer", Geothermics, 87, 101857, https://doi.org/10.1016/j.geothermics.2020.101857

Ungemach, P. (2003): "Reinjection of cooled geothermal brines into sandstone reservoirs", Geothermics, 32-4-6, p. 743-761, https://doi.org/10.1016/S0375-6505(03)00074-9.